

1 Aneuploidy of Specific Chromosomes is Beneficial to Cells Lacking Spindle Checkpoint Protein

2 Bub3

3

4 Pallavi Gadgil¹, Olivia Ballew², Timothy J. Sullivan³, and Soni Lacefield^{1*}

5

6 ¹ Department of Biochemistry and Cell Biology, Geisel School of Medicine at Dartmouth,

7 Hanover, NH, USA

8 ² Department of Biology, Indiana University, Bloomington, Indiana, USA

9 ³ Department of Biomedical Data Science, Geisel School of Medicine at Dartmouth, Hanover,

10 New Hampshire, USA

11

12 Running title: The role of chromosome-specific aneuploidy in Bub3 deficient cells

13

14

15 * Corresponding author

16 Soni.Lacefield@dartmouth.edu

17 74 College St. HB7200

18 Hanover, NH 03755

19 @LacefieldLab

20 Phone:603-646-5896

21 ORC ID: 0000-0002-2862-5067

22

23 **ABSTRACT**

24 Aneuploidy typically poses challenges for cell survival and growth. However, recent studies
25 have identified exceptions where aneuploidy is beneficial for cells with mutations in certain
26 regulatory genes. Our research reveals that cells lacking the spindle checkpoint gene *BUB3*
27 exhibit aneuploidy of select chromosomes. While the spindle checkpoint is not essential in
28 budding yeast, the loss of *BUB3* and *BUB1* increases the probability of chromosome
29 missegregation compared to wildtype cells. Contrary to the prevailing assumption that the
30 aneuploid cells would be outcompeted due to growth defects, our findings demonstrate that
31 *bub3* Δ cells consistently maintained aneuploidy of specific chromosomes over many generations.
32 We investigated whether the persistence of these additional chromosomes in *bub3* Δ cells resulted
33 from the beneficial elevated expression of certain genes, or mere tolerance. We identified several
34 genes involved in chromosome segregation and cell cycle regulation that confer an advantage to
35 Bub3-depleted cells. Overall, our results suggest that the upregulation of specific genes through
36 aneuploidy may provide a survival and growth advantage to strains with poor chromosome
37 segregation fidelity.

38 AUTHOR SUMMARY

39 Accurate chromosome segregation is crucial for the proper development of all living organisms.
40 Errors in chromosome segregation can lead to aneuploidy, characterized by an abnormal number
41 of chromosomes, which generally impairs cell survival and growth. However, under certain
42 stress conditions, such as in various cancers, cells with specific mutations and extra copies of
43 advantageous chromosomes exhibit improved survival and proliferation. In our study, we
44 discovered that cells lacking the spindle checkpoint protein Bub3 became aneuploid, retaining
45 specific chromosomes. This finding was unexpected because although *bub3*Δ cells have a higher
46 rate of chromosome mis-segregation, they were not thought to maintain an aneuploid karyotype.
47 We investigated whether the increased copy number of specific genes on these acquired
48 chromosomes offered a benefit to Bub3-deficient cells. Our results revealed that several genes
49 involved in chromosome segregation and cell cycle regulation prevented the gain of
50 chromosomes upon Bub3-depletion, suggesting that these genes confer a survival advantage.
51 Overall, our study demonstrates that cells lacking Bub3 selectively retain specific chromosomes
52 to increase the copy number of genes that promote proper chromosome segregation.

53 INTRODUCTION

54 Errors in chromosome segregation can give rise to aneuploid cells, which have an
55 abnormal number of chromosomes. Aneuploidy can be deleterious to cells by causing an
56 imbalance in protein expression and proteotoxic stress, which affects both survival and growth
57 [1–4]. Aneuploidy can be particularly detrimental during the development of multicellular
58 organisms. However, there are conditions where aneuploidy provides a benefit to cells, allowing
59 them to grow and divide during stress [5,6]. For example, many pathogenic fungi are aneuploid
60 and chromosome gain can provide drug resistance during infection by increasing the copy
61 number of drug efflux transporters [7]. Similarly, most solid tumors are aneuploid, which likely
62 contributes to cancer progression [8,9]. Finally, although aneuploidy causes growth defects in
63 most budding yeast lab strains, a gain of chromosomes can be beneficial to cells growing in
64 stressful conditions, allowing rapid adaptive evolution [3,4,10]. Furthermore, cells with
65 mutations in some regulatory genes may benefit from aneuploidy [9,11–16]. Therefore, while a
66 high fidelity of chromosome segregation is crucial for survival, allowing occasional errors in
67 segregation may provide a mechanism for adaptation to stressful conditions.

68 Faithful chromosome segregation during mitosis depends on establishing bioriented
69 kinetochore-microtubule attachments, in which the two sister chromatid kinetochores attach to
70 microtubules emanating from opposite spindle poles [17]. Initial attachments are often incorrect
71 with both sister kinetochores attached to the same pole. Error correction mechanisms release
72 incorrect attachments, allowing the establishment of bipolar attachments through cycles of
73 release and reattachment. Additionally, the spindle checkpoint delays the cell cycle in the
74 presence of unattached kinetochores to allow additional time for error correction [18].

75 In budding yeast, the spindle checkpoint is signaled through the action of several non-
76 essential proteins: Mad1, Mad2, Mad3, Bub1, and Bub3 [19–21]. When a kinetochore is
77 unattached, kinetochore protein Spc105/Knl1 becomes phosphorylated, Bub3 and Bub1 bind the
78 kinetochore and recruit Mad1 and Mad2 [19,22]. This interaction ultimately leads to the
79 formation of the diffusible mitotic checkpoint complex (MCC), which consists of Mad2, Mad3,
80 Bub3, and Cdc20 [18,19]. The MCC inhibits the Anaphase Promoting Complex/ Cyclosome
81 (APC/C), a ubiquitin ligase that ubiquitinates proteins and targets them for proteasomal
82 degradation. Inhibition of the APC/C causes cells to arrest at metaphase. Once kinetochores have
83 established bipolar attachments, Spc105/Knl1 is dephosphorylated, the spindle checkpoint
84 proteins are released from the kinetochore, the MCC is disassembled, and anaphase onset ensues.

85 Although the spindle checkpoint proteins are not essential in budding yeast, *bub1Δ* and
86 *bub3Δ* cells are slow-growing and have a prolonged metaphase, unlike *mad1Δ*, *mad2Δ* and
87 *mad3Δ* cells, which grow similarly to wildtype [20,21,23–25]. In addition to their role in spindle
88 checkpoint signaling, Bub3 and Bub1 help recruit Sgo1 to the kinetochore. Sgo1 is important for
89 the biorientation of sister chromatid kinetochores and serves as a platform to recruit other
90 proteins including the chromosome passenger complex (CPC) [26,27]. The CPC contains
91 Ipl1/Aurora kinase B, which is required for error correction of improper kinetochore-microtubule
92 attachments [17]. Ipl1/Aurora B phosphorylates kinetochore proteins to release attachments that
93 are not under tension. In budding yeast, several redundant pathways recruit the CPC to the
94 kinetochore, and therefore, depletion of CPC components has a much more severe phenotype
95 than loss of Bub1 and Bub3 [27–33].

96 Despite the increased rate of chromosome missegregation in *bub1Δ* and *bub3Δ* cells, the
97 previous assumption was that the aneuploid cells would grow slower than the euploid cells and

98 would be outcompeted in the population [23]. However, we noticed that *bub1* Δ and *bub3* Δ cells
99 had an abnormal morphology, prompting us to ask if the aneuploid cells did indeed take over the
100 population. Using a whole genome sequencing approach, we found that *bub3* Δ cells quickly
101 acquired additional copies of one or more of five specific chromosomes: I, II, III, VIII, and X.
102 Over generations, the aneuploidy was persistent yet dynamic, switching between those five
103 chromosomes. We asked which genes on the chromosomes may provide a benefit to the *bub3* Δ
104 cells when the copy number was increased. Our results suggest that several genes, including
105 those involved in chromosome segregation and cell cycle regulation, are advantageous to *bub3* Δ
106 cells when upregulated either individually or in combination. Thus, aneuploidy may be a strategy
107 that allows *bub3* Δ cells to survive and persist despite having lower chromosome segregation
108 fidelity.

109

110 **RESULTS**

111 **The loss of *BUB3* shows the gain of specific chromosomes**

112 Although the spindle checkpoint proteins are not essential in budding yeast, the loss of
113 *bub1* Δ and *bub3* Δ cells have delayed growth, in contrast to *mad1* Δ , *mad2* Δ and *mad3* Δ cells
114 [23,25]. To further characterize the growth delay, we spotted serial dilutions of saturated yeast
115 cultures onto rich media plates. The *bub1* Δ and *bub3* Δ cells showed a growth difference when
116 compared to wildtype, *mad2* Δ , and *mad3* Δ cells (Figure 1A). Growth curves also showed a delay
117 in *bub1* Δ and *bub3* Δ growth compared to wildtype, *mad2* Δ , and *mad3* Δ cells (Figure S1A).
118 Interestingly, we also observed that *bub1* Δ and *bub3* Δ cells had morphological defects, in which
119 the cells were misshaped, larger, elongated, and sometimes formed chains (Figure 1B, S1B). The
120 abnormal morphology prompted us to investigate whether *bub1* Δ and *bub3* Δ cells were

121 aneuploid or had acquired mutations that affected their growth and morphology. The previous
122 assumption was that although *bub3*Δ cells had an increased probability of chromosome
123 missegregation, the aneuploid cells would be outcompeted by the euploid population because
124 they grow slower. We decided to perform further analysis on *bub3*Δ cells because *bub3*Δ cells
125 had a more severe growth defect than *bub1*Δ cells.

126 To determine if the observed growth defects of *bub3*Δ cells were due to chromosome
127 copy number variation (CNV), we performed whole genome sequencing of *bub3*Δ cells. To
128 ensure that we started the experiment with a euploid cell, we deleted one copy of *BUB3* in a
129 wildtype diploid to make a *BUB3/bub3*Δ heterozygote. We induced meiosis in these diploids and
130 then separated the four resulting haploid spores, of which, two were *BUB3* and two were *bub3*Δ
131 (Fig. 1C). From the separated four-spore viable tetrads, the colonies were grown and then kept as
132 frozen stocks. We then recovered the lines and grew them for DNA isolation. This approach
133 minimizes the number of cell division cycles prior to freezing, such that all further experiments
134 are performed on the newly recovered cells from the frozen stocks. We isolated the genomic
135 DNA for whole genome sequencing after the cells underwent approximately 60 cell cycles.

136 We sequenced 11 lines of each genotype, choosing some from the same tetrad and some
137 from different tetrads. The lines had very few mutations, none of which were shared among
138 *bub3*Δ lines (Table S1). As shown in the CNV plots, most of the wildtype strains had one copy
139 of each of the 16 chromosomes (Fig. 1D, Fig. S2A). Although *BUB3* is haplosufficient, there
140 was one tetrad in which both wildtype strains had an additional set of chromosomes XI and XII,
141 likely due to aneuploidy arising in the mitotic divisions prior to meiosis (Fig. S2A).

142 To our surprise, all *bub3*Δ haploids that we sequenced were aneuploid, despite the
143 minimal number of cell divisions prior to sequencing (Fig. 1E, S3A). Of the 16 chromosomes in

144 budding yeast, the gained chromosomes were restricted to chromosomes I, II, III, VIII, and X,
145 with chromosome II present in 8 of the 11 lines (Fig. 2A-B). The lines had between 1-4 extra
146 chromosomes, with most having 2 extra chromosomes (Fig. 2C). These results were unexpected
147 for several reasons. First, we did not expect the rapid accumulation of aneuploidy in the lines, as
148 aneuploidy generally causes a growth disadvantage. Second, while budding yeast can tolerate the
149 aneuploidies of most chromosomes, the consistent accumulation of the same five chromosomes
150 was unexpected [4]. Third, the aneuploid chromosomes varied in size, including both short and
151 long chromosomes, not only the short chromosomes that may be more tolerable. Therefore, we
152 proposed that the gained chromosomes may give *bub3Δ* cells a survival advantage to outcompete
153 the euploid population.

154

155 ***The bub3Δ* lines have a dynamic karyotype over generations**

156 We hypothesized that if the gained chromosomes were beneficial, then *bub3Δ* cells
157 would maintain those chromosomes. Therefore, we asked if the karyotypes of the aneuploid
158 *bub3Δ* lines stabilized after several generations. To this end, we evolved the original wildtype or
159 *bub3Δ* lines by putting them through 20 random bottlenecks, which corresponded to ~460
160 generations (Fig. 3A). The whole genome sequencing showed that the evolved cells acquired few
161 mutations that were not shared among independently evolved clones (Table S1). CNV analysis
162 showed that the wildtype euploid lines maintained their euploid karyotypes, and the wildtype
163 aneuploid lines became less aneuploid, as expected (Fig. 3B, S2B). The evolved *bub3Δ* lines
164 showed the persistence of one or more extra chromosomes, still restricted to chromosomes – I, II,
165 III, VIII, and X (Fig. 2A, 3C, S3B). Strikingly, the karyotypes were dynamic, such that different
166 chromosomes were lost or gained over generations. Evolved lines showed an increased

167 prevalence of chromosome I and were more likely to have 3-4 extra chromosomes than the non-
168 evolved lines (Fig. 2A-C). These results suggest that although the aneuploidy was maintained,
169 the karyotypes did not stabilize, instead, the cells are actively gaining and losing the same 5
170 chromosomes over generations.

171

172 **The evolved *bub3Δ* lines show variable growth rates compared to the non-evolved *bub3Δ*** 173 **lines**

174 The loss of important regulatory genes affects the survival and growth of the cells.
175 Previous studies have shown that cells with mutations in regulatory genes occasionally gain
176 chromosomes or more mutations over time for better survival and growth [9,11–16]. Thus, we
177 hypothesized that the persistent gain of specific chromosomes by evolved *bub3Δ* cells might
178 provide a growth advantage. To test this, we compared the growth of evolved vs non-evolved
179 *bub3Δ* lines to the wildtype lines. To analyze the growth, we diluted the overnight grown cells to
180 OD₆₀₀ of 0.1 and measured the OD₆₀₀ readings for the next 20 hours. The growth curves confirm
181 that the *bub3Δ* lines grow slower as compared to the wildtype and the evolved *bub3Δ* lines do
182 not always grow better than the non-evolved lines (Fig. 3D, Fig. S4A-B). A comparison of the
183 CNV plots and growth curves of *bub3Δ* cells shows that there is neither an obvious correlation
184 between the growth rate and the specific chromosomes gained, nor the number of extra
185 chromosomes (Fig. S4B). These results suggest that the cells undergo chromosomal instability,
186 but still only maintain the same 5 restricted chromosomes (I, II, III, VIII, and X).

187

188 **Loss of Bub3 causes missegregation of other chromosomes, but only specific chromosomes** 189 **are maintained in the population**

190 The gain of these five specific chromosomes in *bub3* Δ cells could be due to either a
191 selective upregulation of the chromosomes or due to the maintenance of chromosomes that were
192 missegregated. To distinguish between these possibilities, we compared the segregation of
193 chromosomes III and IV upon acute Bub3 depletion. We chose these chromosomes because III
194 had an increased copy number in *bub3* Δ lines and IV did not. If the upregulation was selective,
195 we would expect only chromosome III to show an increased copy number in the first cell cycles
196 after Bub3 depletion. In contrast, if there were an equal likelihood of chromosome gain but only
197 specific chromosomes were maintained, we would expect that both III and IV would be
198 upregulated in the first cell cycles after Bub3 depletion.

199 To monitor these chromosomes, we labeled chromosome III or IV with a LacO array and
200 expressed GFP-LacI, which will tag the chromosome with a GFP focus [34]. Cells with one
201 focus in mother and daughter were scored as euploid (Fig. 4A). In contrast, cells with extra GFP
202 foci were scored as aneuploid. To monitor only one cell cycle in the absence of Bub3, we used
203 the anchor away technique to deplete Bub3 from the nucleus upon rapamycin addition [28,29]. In
204 this strain, Bub3 was tagged with FRB (FKBP12-rapamycin binding), and ribosomal protein
205 Rpl13a was tagged with FKBP12 (FK binding protein 12)[35]. With rapamycin binding, FRB
206 and FKBP12 stably interact, resulting in the removal of Bub3 from the nucleus as Rpl13a travels
207 out of the nucleus. The strain also contains *fpr1* Δ and *tor1-1* to allow survival in the presence of
208 rapamycin. We refer to this strain as Bub3-aa (Bub3 anchor away).

209 After synchronizing the cells with the α -factor, we added rapamycin and monitored cells
210 after one cell cycle with Bub3 nuclear depletion. Approximately 4% and 5% of cells
211 missegregated chromosome III and IV, respectively (Fig. 4B). After approximately 18 cell
212 cycles, the percentage of cells with a gain of chromosome III increased significantly. However,

213 the percentage of cells with an additional chromosome IV remained the same. These results
214 suggest that both chromosomes III and IV had an equal likelihood of chromosome
215 missegregation, but only chromosome III was maintained in the population. Overall, this result
216 supports the model that selective increased copy number of chromosome III may provide an
217 advantage to Bub3-depleted cells.

218

219 **Increased expression of *SLI15* and *BIR1* prevents aneuploidy of specific chromosomes**
220 **when Bub3 is depleted from the nucleus**

221 These results led us to hypothesize that increased expression of one or more genes on the
222 aneuploid chromosomes may benefit *bub3* Δ cells, thereby contributing to the retention of these
223 aneuploid chromosomes. If the increased copy number of a gene is advantageous to cells lacking
224 Bub3, we would predict that overexpression of the gene on a plasmid would prevent the retention
225 of the aneuploid chromosome upon Bub3 depletion.

226 To test this prediction, we started our analysis with three genes that encode components
227 of the CPC and are present on the gained chromosomes: *SLI15* (chromosome III), *NBL1*
228 (chromosome VIII), and *BIR1* (chromosome X) (Fig. 4C). We cloned *SLI15*, *NBL1*, and *BIR1*
229 with their endogenous promoters into a centromere-containing (CEN) plasmid and transformed
230 them into the Bub3-aa strain (Fig. 4D). As controls, we also transformed an empty plasmid and a
231 *BUB3*-containing plasmid. We then assessed whether the elevated expression of those genes
232 could prevent aneuploidy of chromosomes I, II, III, VIII, and X (Fig. 4E-I).

233 Consistent with our prior results, approximately 10-15% of cells with the empty plasmid
234 were aneuploid for each chromosome upon Bub3 depletion. The expression of *BUB3* reduced the
235 aneuploidy to approximately 3% upon Bub3 depletion. Elevated expression of *SLI15* and *BIR1*

236 reduced the aneuploidy of the chromosomes containing that specific gene, chromosome II and X
237 to 2-5%, respectively (Fig. 4F, I). In contrast, *NBL1* expression did not decrease the aneuploidy
238 of chromosome VIII (Fig. 4H). Interestingly, *SLI15* expression also reduced aneuploidy of
239 chromosome X and modestly VIII (Fig. 4H-I). *BIR1* expression also reduced aneuploidy of
240 chromosome II and modestly III (Fig. 4F-G). We therefore tested double expression of *SLI15*
241 and *BIR1* and found that the aneuploidy of all 5 chromosomes was reduced (Fig. 4E-I). Overall,
242 these results suggest that increased expression of CPC components *SLI15* and *BIR1* could benefit
243 cells that lack Bub3.

244

245 **Increased expression of several specific genes on chromosome III prevents aneuploidy of** 246 **chromosome III when Bub3 is depleted**

247 Chromosomes I, III, and VIII did not have any obvious candidates for genes that could
248 benefit the *bub3Δ* cells upon upregulation. Because chromosome III is the most highly
249 represented aneuploidy after chromosome II in both the non-evolved and evolved *bub3Δ* strains,
250 we decided to screen for genes on chromosome III that prevent aneuploidy of Bub3-depleted
251 cells. We hypothesized that if increased expression of a specific gene provided a benefit to
252 *bub3Δ* cells, the presence of that gene on a plasmid could prevent the aneuploidy of chromosome
253 III because it would not need to maintain the aneuploidy. We isolated the 2 μ plasmids from the
254 Yeast Tiling Collection that spanned chromosome III, transformed them in Bub3-aa strains
255 individually, and then monitored chromosome III segregation after 18 cell cycles with Bub3
256 nuclear depletion [36]. From this analysis, we found 15 plasmids that could decrease the
257 likelihood of chromosome III gain below 2-fold (there was a 3-fold increased likelihood of
258 chromosome III gain in cells with the empty plasmid as compared to cells with the *BUB3*

259 plasmid; Fig. 5A). Of the 15 plasmids, 3 had overlapping genes. Therefore, we re-tested 12
260 plasmids that reduced chromosome III gain upon Bub3 nuclear depletion (Fig. 5B).

261 We were surprised that so many plasmids reduced chromosome III aneuploidy upon
262 Bub3-depletion. This result suggests that multiple genes likely provide a benefit to cells that lack
263 Bub3. The 2 μ plasmids in the Yeast Tiling Collection contain between 4 to 11 genes in each
264 plasmid (Table S2)[36]. To narrow down the list, we focused on candidates with known roles in
265 chromosome segregation or cell cycle regulation - *BIK1*, *KCC4*, and *CSMI*. We subcloned those
266 genes in *CEN* plasmids and transformed them into Bub3-aa strains. After nuclear depletion of
267 Bub3 for 18 cell cycles, cells expressing *CSMI* did not reduce the percent of cells with
268 chromosome III aneuploidy, suggesting that a different gene on the Tiling plasmid likely reduces
269 the chromosome III aneuploidy. In contrast, elevated expression of *BIK1* and *KCC4* had less
270 aneuploidy of chromosome III than cells with the empty plasmid (Fig 5C). Bik1 is a
271 microtubule-associated protein that is important for chromosome segregation and spindle
272 elongation [31,37–40]. Kcc4 is involved in the G2/M checkpoint [41–43]. Therefore, these genes
273 likely benefit the Bub3-depleted cells by enhancing chromosome segregation.

274 We next asked if the expression of *BIK1* and *KCC4* could prevent the aneuploidy of other
275 chromosomes. We monitored chromosomes I and II and found no significant difference in the
276 percent of aneuploidy upon Bub3 depletion (Fig. 5D-E). However, double expression of both
277 *BIK1* and *KCC4* could prevent aneuploidy of chromosomes II and III, but not I (Fig. 5F-H). We
278 note that expression of both *BIK1* and *KCC4* does not reduce the percent of aneuploidy to levels
279 as low as expression of *BUB3*, suggesting that other genes on that chromosome may also provide
280 a benefit. The double expression of *BIK1* and *SLI15* or *KCC4* and *SLI15* prevented aneuploidy of
281 chromosomes I, II, and III (Fig. 5F-H). This was interesting because the single expression of

282 *SLI15* did not reduce aneuploidy of chromosomes I or III (Fig. 4E, G). These results suggest that
283 there could be synergistic effects from increased expression of specific genes on different
284 chromosomes. Overall, we conclude that by increasing the copy number of the chromosome
285 through aneuploidy, the increased expression of several genes provides *bub3Δ* cells a benefit for
286 growth and survival, allowing cells to maintain those chromosomes.

287

288 **The evolved *bub3Δ* cells maintain aneuploidy after reintroduction of *BUB3***

289 We wondered if the evolved aneuploid *bub3Δ* lines could recover a euploid genotype by
290 adding *BUB3* back to the cells. We tested three evolved *bub3Δ* lines, C2, E3, and G4, and
291 transformed them with a *CEN* plasmid containing *BUB3* (Figure 6A). We then froze them down
292 and struck them out again to grow them up for whole genome sequencing. We purposefully
293 treated them the same as our original assay that identified the *bub3Δ* aneuploid lines after a
294 minimal number of generations, thinking that they would be able to lose the aneuploid
295 chromosomes over the approximately 60 generations if they were no longer providing a benefit
296 to the cells. Surprisingly, the sequencing revealed that all three lines were aneuploid and had
297 different aneuploid karyotypes from the starting evolved lines (Fig. 6B). Although we expected
298 that growth would improve after *BUB3* addition, growth assays showed that strain C2 grew
299 slower after *BUB3* addition, but the other strains showed similar growth with and without *BUB3*
300 addition (Fig. 6C). On a low concentration of the microtubule-depolymerizing drug benomyl,
301 only strain E3 showed better growth upon *BUB3* addition. Overall, these results suggest that the
302 evolved *bub3Δ* cells have a chromosome instability phenotype that was not overcome quickly
303 after adding *BUB3* back.

304

305 **DISCUSSION**

306 Our study reveals that *bub3Δ* haploid cells rapidly gain 5 specific chromosomes in
307 budding yeast: I, II, III, VIII, and X. Most of the lines gained at least 2 chromosomes, with
308 chromosome II highly represented. These chromosomes are a variety of sizes with both long and
309 short chromosomes represented, suggesting that they did not preferentially maintain only the
310 shorter chromosomes. The selective representation of these five chromosomes in *bub3Δ* cells
311 suggests two possibilities: i) these chromosomes were selectively upregulated, or ii) the
312 upregulation of these chromosomes was maintained. We distinguished between these
313 possibilities by comparing the segregation of chromosomes III and IV. Both chromosomes were
314 initially upregulated after Bub3 depletion, but chromosome III was maintained after multiple cell
315 cycles, unlike chromosome IV. These results suggest that all chromosomes have an equal
316 probability of chromosome missegregation, but that only specific chromosomes were
317 maintained. These results led us to hypothesize that the upregulation of these chromosomes may
318 provide a benefit to *bub3Δ* cells, likely due to increased expression of specific genes on those
319 chromosomes.

320 Previous studies have also reported that the upregulation of specific chromosomes occurs
321 in cells that have mutations of different regulatory genes [11–16]. A relevant example analyzed
322 the rare *bir1Δ* survivors [11,15]. Bir1 is an essential component of the CPC, but approximately
323 10% of *bir1Δ* spores can grow into a colony. When these survivors were further evolved, and
324 sequenced, the evolved strains had an increased growth rate, and the same 5 chromosomes were
325 upregulated as found in our study. We found the similarity of upregulating the same 5
326 chromosomes in both *bub3Δ* cells and *bir1Δ* cells surprising because loss of *BIR1* has a much
327 more severe phenotype. Yet, both proteins are involved in recruiting Ipl1/Aurora B to the inner

328 centromere [27]. The *bub3* Δ cells have a less severe phenotype than *bir1* Δ cells because multiple
329 redundant pathways bring the CPC to the kinetochore and the loss of Bub3 only disrupts one of
330 them [27–29]. Furthermore, the evolved *bir1* Δ lines also had additional mutations that were not
331 found in the *bub3* Δ lines, suggesting that these mutations were likely to further help with the
332 survival of *bir1* Δ cells [11,15](Table S1). Combined, these results suggest that there are specific
333 genes whose upregulation provides a mutual benefit to cells with an increased probability of
334 chromosome missegregation.

335 In both *bub3* Δ cells and *bir1* Δ cells, the increased copy number of *SLI15* acquired
336 through the upregulation of chromosome II provided a benefit to the cells [11](Fig. 4).
337 Furthermore, we show that increasing the copy number of CPC component *BIR1* by upregulating
338 chromosome X can also provide a benefit to Bub3-depleted cells (Figure 4). The increased
339 expression of *SLI15* and *BIR1* singly prevents aneuploidy of chromosome II and X upon Bub3
340 depletion. Increased expression of both prevents aneuploidy of all 5 chromosomes upon Bub3
341 depletion. Furthermore, a previous study showed that *bub1* Δ cells cannot survive as tetraploids,
342 but their viability is rescued with increased expression of *BIR1* and *SLI15* [44]. These results
343 suggest that the increased copy number of these two CPC components may provide a benefit by
344 decreasing the probability of chromosome missegregation.

345 The other three chromosomes did not have obvious candidates for genes that when
346 upregulated could potentially provide a benefit to *bub3* Δ cells. We therefore screened all the
347 genes on chromosome III to determine which genes would prevent aneuploidy of chromosome
348 III upon Bub3 depletion. To our surprise, we identified 12 plasmids from the Yeast Tiling
349 Collection that reproducibly prevented aneuploidy (Figure 5A-B). We focused on two potential
350 candidates that had known roles in chromosome segregation or cell cycle regulation: the

351 microtubule-binding protein *BIK1* and a G2/M checkpoint regulator *KCC4* [38–43]. The *BIK1*
352 and *KCC4* single over-expression reduced aneuploidy of chromosome III upon Bub3 depletion,
353 but not of chromosome I or II (Figure 5C-E). The over-expression of both *BIK1* and *KCC4*
354 reduced aneuploidy of the other chromosomes (Figure 5F-H). These results suggest that the
355 increased expression of both *BIK1* and *KCC4* provides an additive benefit to Bub3-depleted
356 cells.

357 Interestingly, when we scanned chromosome III for genes that prevented aneuploidy of
358 chromosome III upon Bub3 depletion, we found 10 other potential candidates in addition to
359 *BIK1* and *KCC4*. There were no other obvious candidates involved in chromosome segregation,
360 but these genes may be involved in other processes that provide an advantage to Bub3-depleted
361 cells and may be interesting to further study. Similarly, besides Nbl1, which did not prevent
362 aneuploidy upon Bub3 depletion, there were no obvious candidates on chromosomes I and VIII.
363 However, our combined results suggest that many genes on chromosomes I, II, III, VIII, and X
364 are likely to provide a benefit to *bub3* Δ cells when upregulated, giving an advantage to the cells
365 that maintain those chromosomes. Therefore, the additive benefits of multiple genes may allow
366 strains with lower chromosome segregation fidelity to survive.

367

368 **MATERIALS AND METHODS**

369 **Yeast and plasmid strains**

370 All *S. cerevisiae* strains are derived from the W303 strain background and are listed in
371 Table S3. All gene deletions, gene tagging, and self-replicating plasmid introductions were
372 performed using the standard PCR-based lithium acetate transformation method [45]. The
373 plasmids to fluorescently tag genes (LacI-GFP and Tub1-mRuby) were integrated into the

374 genome [34,46]. The wildtype or *bub3Δ* haploids used for the evolution were obtained by
375 dissecting tetrads from a *BUB3/bub3Δ* diploid strain (LY4387) to avoid initial aneuploidy. The
376 anchor-away strains have *tor1-1* mutation and *fpr1Δ* to avoid rapamycin toxicity [35]. *RPL13A*
377 was tagged with 2xFKBP12 and *BUB3* was tagged with FRB to allow their interaction in the
378 presence of rapamycin to deplete Bub3 from the nucleus.

379 All plasmids and primers used in this study are listed in Tables S4 and S5, respectively.
380 The CEN overexpression plasmids were cloned using restriction digestion by PCR amplifying
381 the genes of interest with their endogenous promoters from genomic DNA or a Tiling plasmid.
382 The primers had flanking restriction enzyme sites for the cloning (mentioned in Table S5). The
383 PCR products were subcloned in CEN plasmids (Table S4).

384

385 **Media and growth conditions**

386 All yeast strains were grown at 30°C. All yeast strains except the ones transformed with a
387 CEN or 2μ plasmid were grown in media containing 1% yeast extract, 2% peptone, and 2%
388 glucose (YPD). The yeast strains transformed with the Yeast Tiling plasmid collection were
389 grown in YPD supplemented with G418. CEN plasmid-containing yeast strains were grown in
390 synthetic dropout media containing 0.67% yeast nitrogen base without amino acids, 2% glucose
391 (SC), and 0.2% dropout amino acid mix. The Yeast Tiling plasmid collection plasmids (2μ
392 plasmids) were isolated from bacteria grown on LB plates (or media) supplemented with
393 50μg/mL of kanamycin [36]. The other bacterial plasmids were grown on LB plates (or media)
394 supplemented with 100μg/mL of ampicillin. The plasmids were isolated using QIAprep® Spin
395 Miniprep kit.

396

397 **Evolution of wildtype or mutant *BUB3* haploids**

398 To minimize aneuploidy, we used a wildtype diploid and then deleted one copy of *BUB3*
399 to get a heterozygous *BUB3/bub3::LEU2* diploid (LY4387). We sporulated the diploids and then
400 dissected the tetrads. The 4-spore viable tetrads were grown up in YPD and frozen. They were
401 then restreaked and grown up in YPD for genomic DNA preparation for sequencing. To obtain
402 the evolved wildtype or *bub3*Δ cells, the non-evolved strains underwent 20 random bottlenecks
403 in which the plates were marked prior to streaking and colonies closest to the mark were
404 restreaked for the next bottleneck, allowing a random selection of the colonies. The 20 passages
405 account for approximately 460 generations. The evolved strains were grown up for freezing and
406 then restreaked and grown up for genomic DNA preparation for sequencing.

407

408 **Whole Genome Sequencing analysis**

409 Library preparation

410 Input DNA was quantified by Qubit (Thermo Fisher) and 200ng was used as input into
411 the Nextera DNA with tagmentation workflow (Illumina) to generate Illumina sequencing
412 libraries according to the manufacturer's protocol. Libraries were normalized and pooled for
413 sequencing on a NextSeq2000 (Illumina), targeting 10 million, 150bp paired-end reads per
414 sample.

415 Read Alignment

416 Raw reads were trimmed with Trimmomatic v0.39 [47], with the following parameters,
417 “ILLUMINACLIP:TruSeq3-PE-2.fa:2:30:10:2:keepBothReads LEADING:3 TRAILING:3
418 MINLEN:36”. Trimmed reads were aligned to the Yeast genome S288C, available at NCBI

419 accession GCF_000146045.2, using BWA 0.7.17 [48], with default parameters. Duplicate reads
420 were marked with “MarkDuplicates” from Picard tools v2.27.1, with default parameters.

421 SNP and Indel Analysis

422 SNPs and small indels were called with FreeBayes v1.3.4 [49] and the following
423 parameters “--min-coverage 5 --limit-coverage 200 --min-alternate-fraction .2 --min-mapping-
424 quality 15 --min-alternate-count 2”. SNPs were annotated using SNPEff v5.0e [50].

425 Copy Number Analysis

426 Copy number analysis was performed using the following commands from the Genome
427 Analysis Tool Kit (GATK) v4.5.0.0 [51]. Genome intervals for calculating copy number were
428 determined with the PreprocessIntervals command, with the following parameters, “--padding 0 -
429 imr OVERLAPPING_ONLY”. Reads counts for each sample and each interval were collected
430 using the CollectReadCounts command, with default parameters. Copy number per interval was
431 standardized and denoised using the DenoiseReadCounts command, with the “--standardized-
432 copy-ratios” and “--denoised-copy-ratios” parameters. Genome-wide copy number graphs were
433 created by plotting columns 2 (“START”) and 4 (“LOG2_COPY_RATIO”) of the denoised copy
434 ratio output.

435

436 **Spot assay**

437 For spot assays, the strains were grown in YPD for 18-20hrs at 30°C. The saturated
438 cultures were serially diluted 1:10 and spotted on YPD plates and incubated at 30°C for 40 hours.

439

440 **Growth curve analysis**

441 Strains were grown in YPD for 18-20hrs at 30°C. The cultures were diluted to 0.1 OD₆₀₀
442 in YPD. OD₆₀₀ readings were taken with the Synergy Neo2 plate reader every 10 minutes in
443 triplicates for approximately 20 hours.

444

445 **Overexpression screen for chromosome III genes**

446 The Yeast Tiling Collection plasmids were isolated and 96-well plate transformations
447 were performed as follows [36,52]. LY9391 was grown in 20mL of YPD for 12 hours at 30°C.
448 2.5×10^8 cells were transferred to 50ml of pre-warmed YPD and incubated at 30°C for 4 hours.
449 The culture was spun down and the pellet was resuspended in 15mL of media. 200μL of cells
450 were transferred to 96-well plates and the plates were centrifuged for 10 minutes at 1300g. The
451 supernatant was discarded. 5μL of the Yeast Genomic Tiling Collection plasmids were added to
452 each well. 35μL of the transformation mix (15μL of 1M lithium acetate + 20μL of boiled
453 2mg/mL single-stranded salmon sperm DNA) and 100μL of 50% PEG (MW 3350) were added
454 to the cell pellet and incubated at 42°C for 2 hours. The plate was centrifuged at 1300g for 10
455 minutes. The supernatant was discarded and 10μL of sterile water was added to the cells and
456 5μL of cells were spotted on SC-leu plates. The plates were incubated at 30°C for 24 hours and
457 then replica-plated on YPD+G418 plates for 2-4 days at 30°C. The single colonies obtained from
458 the transformation were restreaked on YPD+G418 and then grown up and frozen down. For the
459 overexpression assay, cells were recovered from the frozen stocks, and then grown on
460 YPD+G418 plates with or without rapamycin (1μg/ml) for 24 hours at 30°C. A random single
461 colony was incubated in YPD+G418 media with or without rapamycin (1μg/mL) for 6 hours at
462 30°C. The culture was spun down and washed with SC media. 500 cells were scored in each
463 sample as either euploid or aneuploid using LacO-LacI-GFP foci.

464

465 **Overexpression screen for individual genes**

466 To analyze the effect of overexpression of CPC genes and chromosome III candidates
467 obtained from the overexpression screen, the genes of interest were cloned in a CEN-plasmid as
468 listed in Table S4 and transformed in yeast strains containing LacO arrays on the chromosomes
469 of interest as listed in Table S3. The frozen stocks of the transformed yeast strains were
470 recovered on appropriate SC dropout plates and a random fully grown colony was streaked on
471 plates with and without Rapamycin (1 µg/mL) for 24 hours at 30°C. A random single colony was
472 incubated in appropriate SC dropout media with or without Rapamycin (1 µg/mL) for 6 hours at
473 30°C. 500 cells were scored for each sample as either euploid or aneuploid using LacO-LacI-
474 GFP foci.

475

476 **Statistical analysis**

477 The statistical analysis for all graphs was done using GraphPad Prism 10.2.2. The two-
478 tailed P values were calculated using the unpaired t-test with Welch's correction. The
479 significance is as follows: **** < 0.0001, *** < 0.001, ** < 0.01, ns > 0.05.

480

481 **ACKNOWLEDGEMENTS**

482 We thank the Lacefield lab for comments on the manuscript. We thank Sue Biggins for strains.
483 Whole Genome Sequencing for SNP and CNV analysis was carried out in the Genomics and
484 Molecular Biology Shared Resource (RRID:SCR021293) at Dartmouth which is supported by
485 NCI Cancer Center Support Grant 5P30CA023108 and NIH S10 (1S10OD030242) awards.

486 The work is supported by the bioMT core facility through P20-GM113132 and through NIGMS
487 grant R01GM105755 to SL.

488

489 REFERENCES

- 490 1. Donnelly N, Storchová Z. Aneuploidy and proteotoxic stress in cancer. *Mol Cell Oncol.*
491 2015;2: e976491. doi:10.4161/23723556.2014.976491
- 492 2. Oromendia AB, Dodgson SE, Amon A. Aneuploidy causes proteotoxic stress in yeast. *Genes*
493 *Dev.* 2012;26: 2696–2708. doi:10.1101/gad.207407.112
- 494 3. Pavelka N, Rancati G, Zhu J, Bradford WD, Saraf A, Florens L, et al. Aneuploidy confers
495 quantitative proteome changes and phenotypic variation in budding yeast. *Nature.* 2010;468:
496 321–325. doi:10.1038/nature09529
- 497 4. Torres EM, Sokolsky T, Tucker CM, Chan LY, Boselli M, Dunham MJ, et al. Effects of aneuploidy
498 on cellular physiology and cell division in haploid yeast. *Science.* 2007;317: 916–924.
499 doi:10.1126/science.1142210
- 500 5. Nicholson JM, Cimini D. Cancer karyotypes: survival of the fittest. *Front Oncol.* 2013;3: 148.
501 doi:10.3389/fonc.2013.00148
- 502 6. Pavelka N, Rancati G, Li R. Dr Jekyll and Mr Hyde: role of aneuploidy in cellular adaptation and
503 cancer. *Curr Opin Cell Biol.* 2010;22: 809–815. doi:10.1016/j.ceb.2010.06.003
- 504 7. Kwon-Chung KJ, Chang YC. Aneuploidy and drug resistance in pathogenic fungi. *PLoS Pathog.*
505 2012;8: e1003022. doi:10.1371/journal.ppat.1003022
- 506 8. Wang Z, Xia Y, Mills L, Nikolakopoulos AN, Maeser N, Dehm SM, et al. Evolving copy number
507 gains promote tumor expansion and bolster mutational diversification. *Nat Commun.* 2024;15:
508 2025. doi:10.1038/s41467-024-46414-5
- 509 9. Klockner TC, Campbell CS. Selection forces underlying aneuploidy patterns in cancer. *Mol Cell*
510 *Oncol.* 2024;11: 2369388. doi:10.1080/23723556.2024.2369388
- 511 10. Torres EM. Consequences of gaining an extra chromosome. *Chromosome Res.* 2023;31: 24.
512 doi:10.1007/s10577-023-09732-w
- 513 11. Ravichandran MC, Fink S, Clarke MN, Hofer FC, Campbell CS. Genetic interactions between
514 specific chromosome copy number alterations dictate complex aneuploidy patterns. *Genes*
515 *Dev.* 2018;32: 1485–1498. doi:10.1101/gad.319400.118
- 516 12. Chen G, Bradford WD, Seidel CW, Li R. Hsp90 stress potentiates rapid cellular adaptation
517 through induction of aneuploidy. *Nature.* 2012;482: 246–250. doi:10.1038/nature10795

- 518 13. Ryu H-Y, Wilson NR, Mehta S, Hwang SS, Hochstrasser M. Loss of the SUMO protease Ulp2
519 triggers a specific multichromosome aneuploidy. *Genes Dev.* 2016;30: 1881–1894.
520 doi:10.1101/gad.282194.116
- 521 14. Adell MAY, Klockner TC, Höfler R, Wallner L, Schmid J, Markovic A, et al. Adaptation to spindle
522 assembly checkpoint inhibition through the selection of specific aneuploidies. *Genes Dev.*
523 2023;37: 171–190. doi:10.1101/gad.350182.122
- 524 15. Clarke MN, Marsoner T, Adell MAY, Ravichandran MC, Campbell CS. Adaptation to high rates of
525 chromosomal instability and aneuploidy through multiple pathways in budding yeast. *EMBO J.*
526 2023;42: e111500. doi:10.15252/embj.2022111500
- 527 16. Kaya A, Gerashchenko MV, Seim I, Labarre J, Toledano MB, Gladyshev VN. Adaptive aneuploidy
528 protects against thiol peroxidase deficiency by increasing respiration via key mitochondrial
529 proteins. *Proc Natl Acad Sci U S A.* 2015;112: 10685–10690. doi:10.1073/pnas.1505315112
- 530 17. Tanaka TU, Zhang T. SWAP, SWITCH, and STABILIZE: Mechanisms of Kinetochores-Microtubule
531 Error Correction. *Cells.* 2022;11: 1462. doi:10.3390/cells11091462
- 532 18. Musacchio A. The Molecular Biology of Spindle Assembly Checkpoint Signaling Dynamics. *Curr*
533 *Biol.* 2015;25: R1002-1018. doi:10.1016/j.cub.2015.08.051
- 534 19. Lara-Gonzalez P, Pines J, Desai A. Spindle assembly checkpoint activation and silencing at
535 kinetochores. *Semin Cell Dev Biol.* 2021;117: 86–98. doi:10.1016/j.semcdb.2021.06.009
- 536 20. Li R, Murray AW. Feedback control of mitosis in budding yeast. *Cell.* 1991;66: 519–531.
537 doi:10.1016/0092-8674(81)90015-5
- 538 21. Hoyt MA, Totis L, Roberts BT. *S. cerevisiae* genes required for cell cycle arrest in response to
539 loss of microtubule function. *Cell.* 1991;66: 507–517. doi:10.1016/0092-8674(81)90014-3
- 540 22. Primorac I, Weir JR, Chirolì E, Gross F, Hoffmann I, van Gerwen S, et al. Bub3 reads
541 phosphorylated MELT repeats to promote spindle assembly checkpoint signaling. *Elife.* 2013;2:
542 e01030. doi:10.7554/eLife.01030
- 543 23. Warren CD, Brady DM, Johnston RC, Hanna JS, Hardwick KG, Spencer FA. Distinct
544 chromosome segregation roles for spindle checkpoint proteins. *Mol Biol Cell.* 2002;13: 3029–
545 3041. doi:10.1091/mbc.e02-04-0203
- 546 24. Yang Y, Lacefield S. Bub3 activation and inhibition of the APC/C. *Cell Cycle.* 2016;15: 1–2.
547 doi:10.1080/15384101.2015.1106746
- 548 25. Yang Y, Tsuchiya D, Lacefield S. Bub3 promotes Cdc20-dependent activation of the APC/C in *S.*
549 *cerevisiae*. *J Cell Biol.* 2015;209: 519–527. doi:10.1083/jcb.201412036
- 550 26. Kawashima SA, Yamagishi Y, Honda T, Ishiguro K, Watanabe Y. Phosphorylation of H2A by
551 Bub1 prevents chromosomal instability through localizing shugoshin. *Science.* 2010;327: 172–
552 177. doi:10.1126/science.1180189

- 553 27. Cairo G, Lacefield S. Establishing correct kinetochore-microtubule attachments in mitosis and
554 meiosis. *Essays Biochem.* 2020;64: 277–287. doi:10.1042/EBC20190072
- 555 28. Cairo G, Greiwe C, Jung GI, Blengini C, Schindler K, Lacefield S. Distinct Aurora B pools at the
556 inner centromere and kinetochore have different contributions to meiotic and mitotic
557 chromosome segregation. *Mol Biol Cell.* 2023;34: ar43. doi:10.1091/mbc.E23-01-0014
- 558 29. Cairo G, MacKenzie AM, Lacefield S. Differential requirement for Bub1 and Bub3 in regulation
559 of meiotic versus mitotic chromosome segregation. *J Cell Biol.* 2020;219: e201909136.
560 doi:10.1083/jcb.201909136
- 561 30. Cho U-S, Harrison SC. Ndc10 is a platform for inner kinetochore assembly in budding yeast.
562 *Nat Struct Mol Biol.* 2011;19: 48–55. doi:10.1038/nsmb.2178
- 563 31. Edgerton H, Johansson M, Keifenheim D, Mukherjee S, Chacón JM, Bachant J, et al. A
564 noncatalytic function of the topoisomerase II CTD in Aurora B recruitment to inner centromeres
565 during mitosis. *J Cell Biol.* 2016;213: 651–664. doi:10.1083/jcb.201511080
- 566 32. Fischböck-Halwachs J, Singh S, Potocnjak M, Hagemann G, Solis-Mezarino V, Woike S, et al.
567 The COMA complex interacts with Cse4 and positions Slh15/Ipl1 at the budding yeast inner
568 kinetochore. *Elife.* 2019;8: e42879. doi:10.7554/eLife.42879
- 569 33. García-Rodríguez LJ, Kasciukovic T, Denninger V, Tanaka TU. Aurora B-INCENP Localization at
570 Centromeres/Inner Kinetochores Is Required for Chromosome Bi-orientation in Budding Yeast.
571 *Curr Biol.* 2019;29: 1536-1544.e4. doi:10.1016/j.cub.2019.03.051
- 572 34. Straight AF, Belmont AS, Robinett CC, Murray AW. GFP tagging of budding yeast chromosomes
573 reveals that protein-protein interactions can mediate sister chromatid cohesion. *Curr Biol.*
574 1996;6: 1599–1608. doi:10.1016/s0960-9822(02)70783-5
- 575 35. Haruki H, Nishikawa J, Laemmli UK. The anchor-away technique: rapid, conditional
576 establishment of yeast mutant phenotypes. *Mol Cell.* 2008;31: 925–932.
577 doi:10.1016/j.molcel.2008.07.020
- 578 36. Jones GM, Stalker J, Humphray S, West A, Cox T, Rogers J, et al. A systematic library for
579 comprehensive overexpression screens in *Saccharomyces cerevisiae*. *Nat Methods.* 2008;5:
580 239–241. doi:10.1038/nmeth.1181
- 581 37. Lin H, de Carvalho P, Kho D, Tai CY, Pierre P, Fink GR, et al. Polyploids require Bik1 for
582 kinetochore-microtubule attachment. *J Cell Biol.* 2001;155: 1173–1184.
583 doi:10.1083/jcb.200108119
- 584 38. Berlin V, Styles CA, Fink GR. BIK1, a protein required for microtubule function during mating
585 and mitosis in *Saccharomyces cerevisiae*, colocalizes with tubulin. *J Cell Biol.* 1990;111: 2573–
586 2586. doi:10.1083/jcb.111.6.2573
- 587 39. Raspelli E, Facchinetti S, Fraschini R. Swe1 and Mih1 regulate mitotic spindle dynamics in
588 budding yeast via Bik1. *J Cell Sci.* 2018;131: jcs213520. doi:10.1242/jcs.213520

- 589 40. Julner A, Abbasi M, Menéndez-Benito V. The microtubule plus-end tracking protein Bik1 is
590 required for chromosome congression. *Mol Biol Cell*. 2022;33: br7. doi:10.1091/mbc.E21-10-
591 0500
- 592 41. Barral Y, Parra M, Bidlingmaier S, Snyder M. Nim1-related kinases coordinate cell cycle
593 progression with the organization of the peripheral cytoskeleton in yeast. *Genes Dev*. 1999;13:
594 176–187. doi:10.1101/gad.13.2.176
- 595 42. Okuzaki D, Nojima H. Kcc4 associates with septin proteins of *Saccharomyces cerevisiae*. *FEBS*
596 *Lett*. 2001;489: 197–201. doi:10.1016/s0014-5793(01)02104-4
- 597 43. Okuzaki D, Watanabe T, Tanaka S, Nojima H. The *Saccharomyces cerevisiae* bud-neck proteins
598 Kcc4 and Gin4 have distinct but partially-overlapping cellular functions. *Genes Genet Syst*.
599 2003;78: 113–126. doi:10.1266/ggs.78.113
- 600 44. Storchová Z, Becker JS, Talarek N, Kögelsberger S, Pellman D. Bub1, Sgo1, and Mps1 mediate a
601 distinct pathway for chromosome biorientation in budding yeast. *Mol Biol Cell*. 2011;22: 1473–
602 1485. doi:10.1091/mbc.E10-08-0673
- 603 45. Janke C, Magiera MM, Rathfelder N, Taxis C, Reber S, Maekawa H, et al. A versatile toolbox for
604 PCR-based tagging of yeast genes: new fluorescent proteins, more markers and promoter
605 substitution cassettes. *Yeast*. 2004;21: 947–962. doi:10.1002/yea.1142
- 606 46. Markus SM, Omer S, Baranowski K, Lee W-L. Improved Plasmids for Fluorescent Protein
607 Tagging of Microtubules in *Saccharomyces cerevisiae*. *Traffic*. 2015;16: 773–786.
608 doi:10.1111/tra.12276
- 609 47. Bolger AM, Lohse M, Usadel B. Trimmomatic: a flexible trimmer for Illumina sequence data.
610 *Bioinformatics*. 2014;30: 2114–2120. doi:10.1093/bioinformatics/btu170
- 611 48. Li H, Durbin R. Fast and accurate long-read alignment with Burrows-Wheeler transform.
612 *Bioinformatics*. 2010;26: 589–595. doi:10.1093/bioinformatics/btp698
- 613 49. Garrison E, Marth G. Haplotype-based variant detection from short-read sequencing. *arXiv*;
614 2012. doi:10.48550/arXiv.1207.3907
- 615 50. Cingolani P, Platts A, Wang LL, Coon M, Nguyen T, Wang L, et al. A program for annotating and
616 predicting the effects of single nucleotide polymorphisms, SnpEff: SNPs in the genome of
617 *Drosophila melanogaster* strain w1118; iso-2; iso-3. *Fly (Austin)*. 2012;6: 80–92.
618 doi:10.4161/fly.19695
- 619 51. McKenna A, Hanna M, Banks E, Sivachenko A, Cibulskis K, Kernytsky A, et al. The Genome
620 Analysis Toolkit: a MapReduce framework for analyzing next-generation DNA sequencing data.
621 *Genome Res*. 2010;20: 1297–1303. doi:10.1101/gr.107524.110
- 622 52. Gavade JN, Lacefield S. High-throughput genetic screening of meiotic commitment using
623 fluorescence microscopy in *Saccharomyces cerevisiae*. *STAR Protoc*. 2022;3: 101797.
624 doi:10.1016/j.xpro.2022.101797

625

626 **FIGURE LEGENDS**

627

628 **Figure 1. Loss of *BUB3* causes growth, morphological, and chromosome segregation**
629 **defects.**

630 **(A)** Comparison of growth of wildtype and spindle checkpoint deleted strains. Saturated yeast
631 cultures were serially diluted, spotted on YPD plates, and imaged after 40 hours of incubation.

632 **(B)** Representative DIC images of the morphological differences between wildtype and *bub3Δ*
633 cells. Scale bar = 5μm. **(C)** Schematic of obtaining haploids for whole genome sequencing after

634 60 generations of growth. **(D, E)** The CNV plots of wildtype (D) or *bub3Δ* (E) cells. The x-axis
635 shows the 16 budding yeast chromosomes separated by vertical dotted lines according to size.

636 They y-axis shows $\log_2(\text{copy number})$. The horizontal dotted line delineates 1 chromosome copy.
637 Each increment shows an additional chromosome copy.

638

639 **Figure 2. *bub3Δ* cells have unstable karyotypes with a chromosome gain bias.**

640 **(A)** Table of chromosomes gained in the non-evolved and evolved *bub3Δ* lines obtained from
641 whole genome sequencing. The chromosomes with a 1.5-fold increase are in parentheses. **(B)**

642 Graph comparing 2-fold (solid bars) or 1.5-fold (patterned bars) upregulation of the different
643 chromosomes in the non-evolved (grey) and evolved (orange) *bub3Δ* lines. **(C)** Graph of the

644 percent of *bub3Δ* lines with the listed number of extra copies of the chromosomes.

645

646 **Figure 3 - Evolved *bub3Δ* lines continue to gain one or more specific chromosomes that do**
647 **not always cause a growth advantage.**

648 (A) Workflow of the evolution of wildtype or *bub3Δ* lines for whole genome sequencing after
649 460 generations. (B-C) CNV plots of wildtype (B) or *bub3Δ* (C) karyotypes. The x-axis shows
650 the 16 budding yeast chromosomes separated by vertical dotted lines according to their sizes.
651 The y-axis shows the \log_2 (copy number). The horizontal line signifies 1 chromosome copy, and
652 each increment shows an additional chromosome copy. (D) Growth curves comparing evolved
653 (dotted lines) vs non-evolved (solid lines) *bub3Δ* lines to a wildtype strain (in grey). The cells
654 were grown to saturation, diluted to 0.1 OD₆₀₀ and then the OD₆₀₀ was measure for 20 hours.

655

656 **Figure 4. Overexpression of *SLI15* and *BIR1* prevents aneuploidy of specific chromosomes**
657 **upon Bub3 depletion.**

658 (A) Representative images of euploid and aneuploid cells. Cells express LacI-GFP and LacO
659 repeats are placed on chromosome III (first two images) and chromosome I (third image). Scale
660 bar = 5 μ m. (B) Graph comparing the percent aneuploidy of chromosomes III and IV after the 1st
661 (light brown bars) and 18th (dark brown bars) cell cycle after Bub3 depletion (n \geq 500 cells per
662 replicate; significance with unpaired t-test with Welch's correction, error bars show standard
663 deviation). (C) Schematic of the chromosomes upregulated in *bub3Δ* lines with genes of interest
664 marked. The sizes are comparable by scale. (D) Workflow of the overexpression screen. (E-I)
665 Graphs of the percent aneuploidy of Bub3-aa strains with overexpression of CPC members
666 *SLI15* (green), *BIR1* (pink), and *NBL1* (olive green) and with *SLI15* and *BIR1* combined (green
667 with pink pattern) compared to strains with the control plasmids pEmpty (in purple) and p*BUB3*
668 (in grey) comparing chromosomes I (E), II (F), III (G), VIII (H), and X (I) (n \geq 500 cells each
669 replicate; significance with unpaired t-test with Welch's correction; error bars represent standard
670 deviation).

671
672 **Figure 5. Elevated expression of a subset of genes from chromosome III prevents the gain**
673 **of chromosome III upon Bub3 depletion.**
674 **(A)** Graph comparing the fold-change in chromosome III gain for Bub3-aa strains with the
675 plasmids of interest (x-axis) from the Yeast Tiling plasmid collection that spans chromosome III,
676 *pBUB3* (dark grey) and *pEmpty* (purple) ($n \geq 500$ cells per line). The dotted line shows the cut-
677 off of short-listed candidate plasmids. **(B)** The graphs showing the secondary screen of the short-
678 listed candidates. Plasmids with the genes of interest are marked with an arrow. **(C, D, E, F)**
679 Graph of the percent aneuploidy for Bub3-aa strains with overexpression of the genes of interest
680 **(C)** *BIK1*, *KCC4*, and *CSMI* for chromosome III; **(D, E)** *BIK1* and *KCC4* for chromosome I and
681 II; **(F)** double overexpression of the genes of interest for chromosomes I, II, III ($n \geq 500$ cells for
682 each replicate; significance with unpaired t-test with Welch's correction; error bars represent
683 SD).

684
685 **Figure 6. The re-introduction of *BUB3* in evolved *bub3Δ* lines does not rescue aneuploidy.**
686 **(A)** Workflow for *BUB3* reintroduction in evolved *bub3Δ* lines for whole genome sequencing.
687 **(B)** CNV plots comparing the evolved *bub3Δ* lines with and without the rescue plasmid. **(C)**
688 Growth curve comparing the evolved *bub3Δ* lines and a wildtype line before and after addition
689 of the rescue plasmid. **(D)** 1:10 serial dilutions of saturated cultures comparing the benomyl
690 sensitivity of evolved *bub3Δ* lines with and without *pBUB3* (5 μ g/mL of benomyl).

691
692 **Figure S1. Spindle checkpoint mutants differentially affect cellular growth and**
693 **morphology.**

694 **(A)** Growth curves comparing wildtype and individual spindle checkpoint deletion strains. **(B)**
695 Representative DIC images comparing morphological differences of wildtype and spindle
696 checkpoint mutant strains (scale bar = 5 μ m).

697

698 **Figure S2. Wildtype lines maintain normal chromosome copy numbers.**

699 **(A, B)** The CNV plots of wildtype non-evolved (A) and evolved (B) lines. The x-axis shows the
700 16 yeast chromosomes spaced by vertical dotted lines according to their sizes. The horizontal
701 dotted line shows 1 chromosome copy. Each increment shows an additional chromosome copy.

702

703 **Figure S3. *bub3* Δ lines have varying chromosome copy numbers over time.**

704 **(A, B)** The CNV of *bub3* Δ non-evolved (A) and evolved (B) lines. The x-axis shows the 16
705 budding yeast chromosomes spaced by vertical dotted lines according to their sizes. The
706 horizontal dotted line shows 1 chromosome copy. Each increment shows an additional
707 chromosome copy.

708

709 **Figure S4. The evolution of *bub3* Δ lines does not always provide a growth advantage.**

710 **(A)** Growth curves comparing evolved (dotted lines) to non-evolved (solid lines) wildtype and
711 *bub3* Δ lines. **(B)** Table comparing the growth pattern and the gain of chromosomes for non-
712 evolved and evolved *bub3* Δ lines. Growth is marked as better (+), similar (\pm), and worse (-).

Figure 1

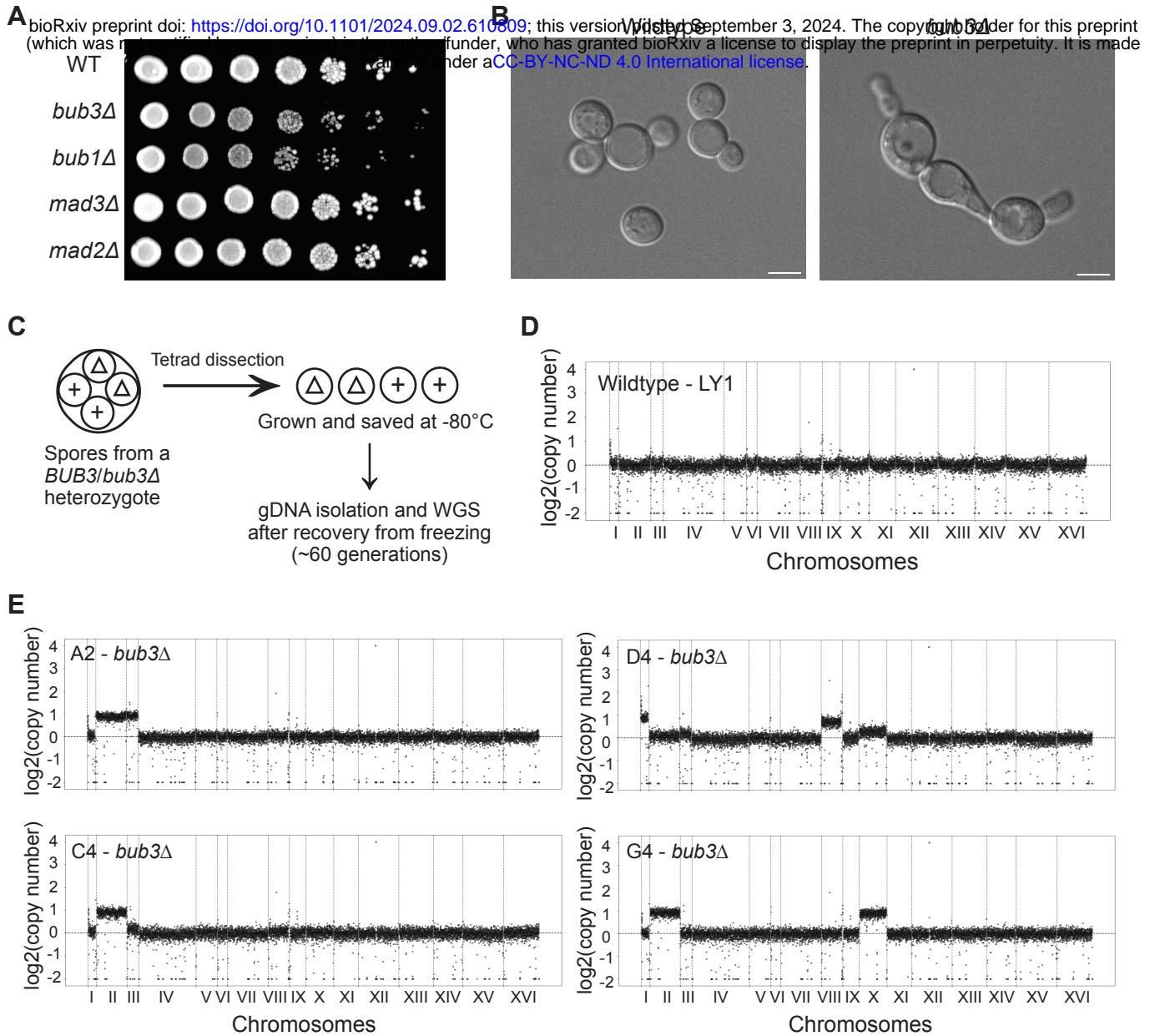


Figure 2

bioRxiv preprint doi: <https://doi.org/10.1101/2024.09.02.610809>; this version posted September 3, 2024. The copyright holder for this preprint (which was not certified by peer review) is the author/funder, who has granted bioRxiv a license to display the preprint in perpetuity. It is made available under a [CC-BY-NC-ND 4.0 International license](https://creativecommons.org/licenses/by-nc-nd/4.0/).

	Haploid	Gain of chromosomes	
		non-evolved <i>bub3Δ</i>	evolved <i>bub3Δ</i>
1	A2	II, III	II (I, III, VIII)
2	A3	X (VIII)	II, VIII
3	B3	II, III	I (X)
4	C2	II	I, III
5	C4	II (III)	II, VIII (III)
6	D2	I, II	II
7	D4	I, VIII (III, X)	VIII, X (I, III)
8	E3	II, III (X)	I, II, III
9	E4	VIII, X	II, III
10	F4	II, III	I, X (II)
11	G4	II, X	I, II, III

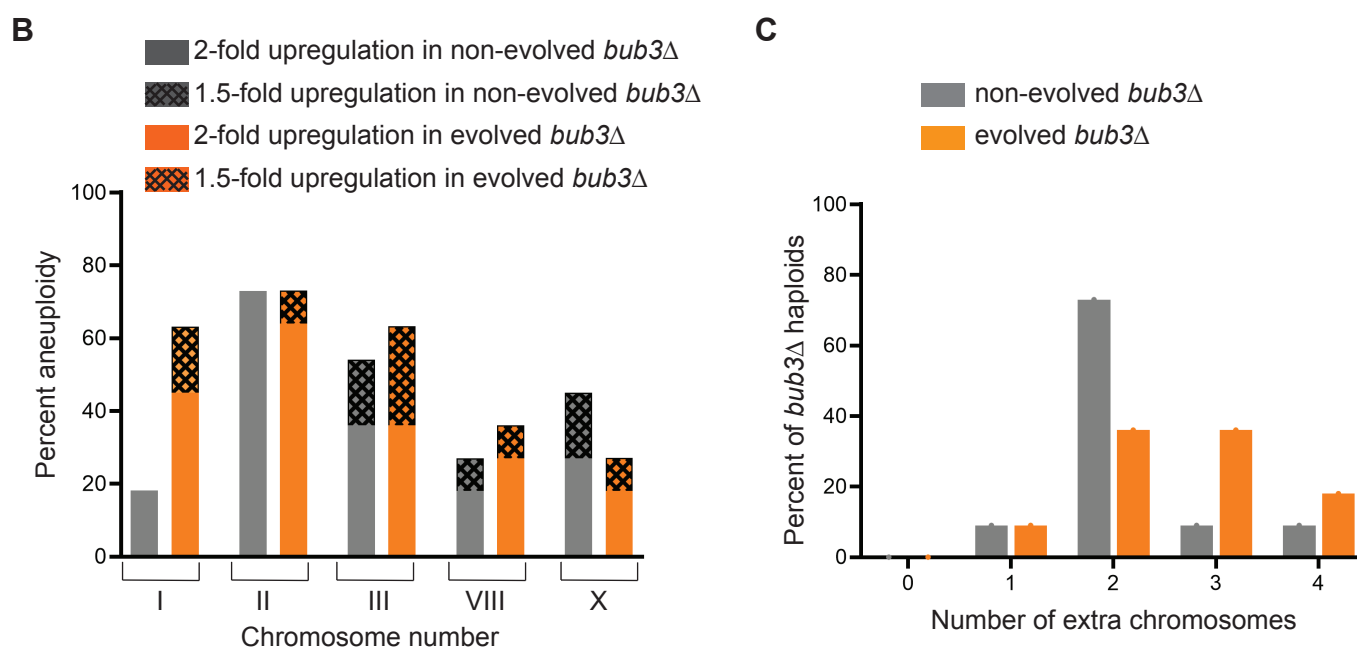


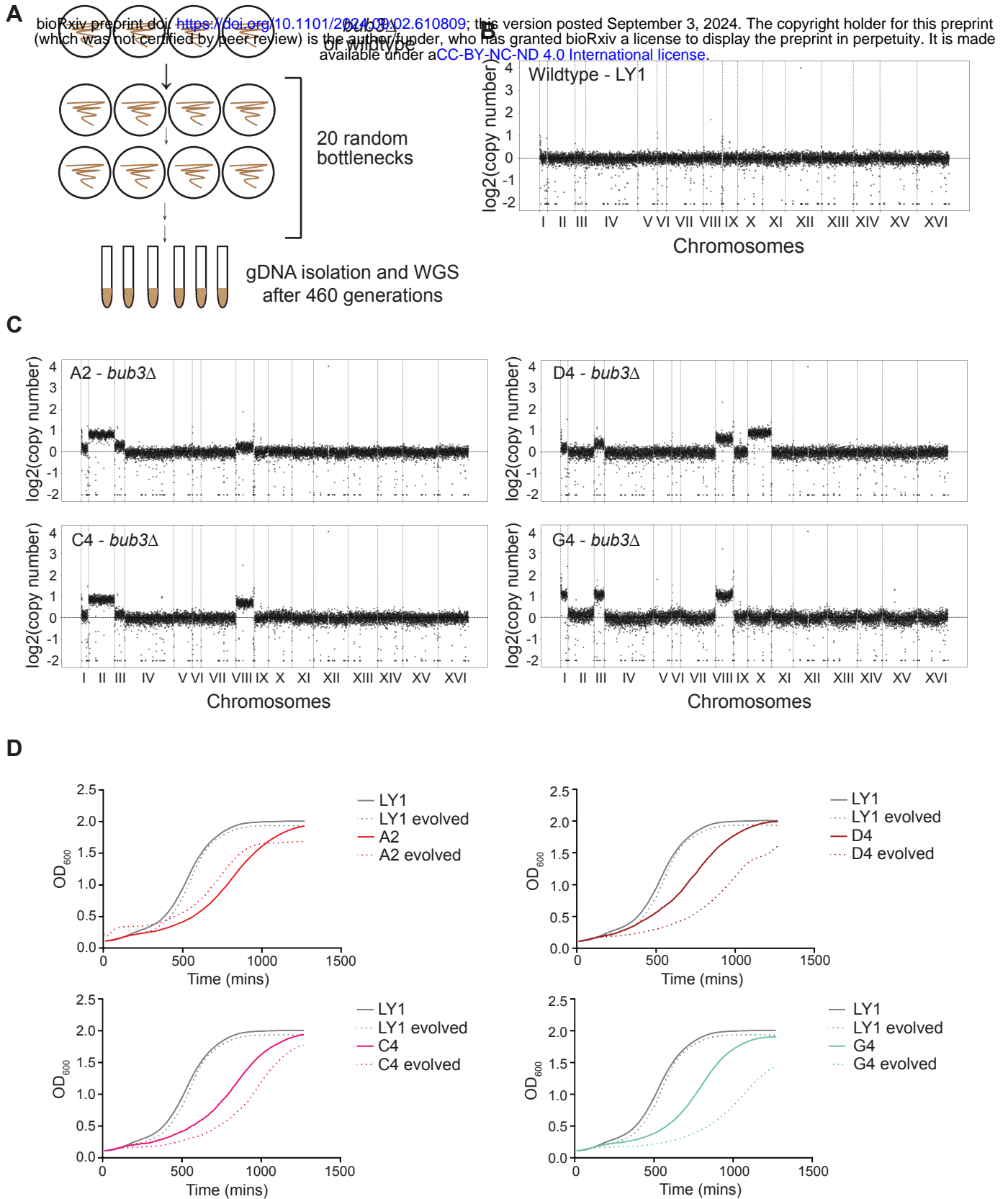
Figure 3

Figure 4

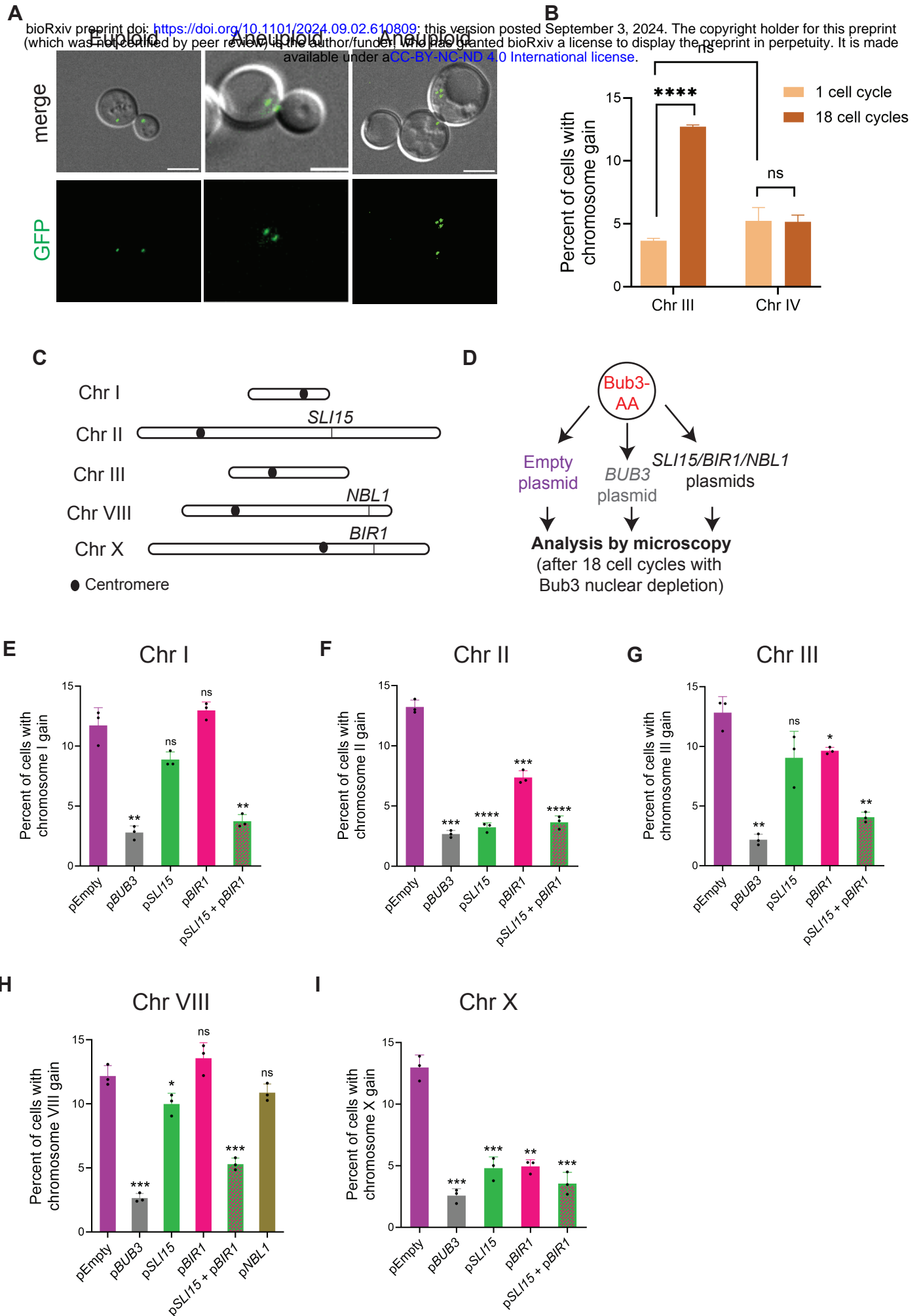


Figure 5**A**

bioRxiv preprint doi: <https://doi.org/10.1101/2024.09.02.610809>; this version posted September 3, 2024. The copyright holder for this preprint (which was not certified by peer review) is the author/funder, who has granted bioRxiv a license to display the preprint in perpetuity. It is made available under a [CC-BY-NC-ND 4.0 International license](#).

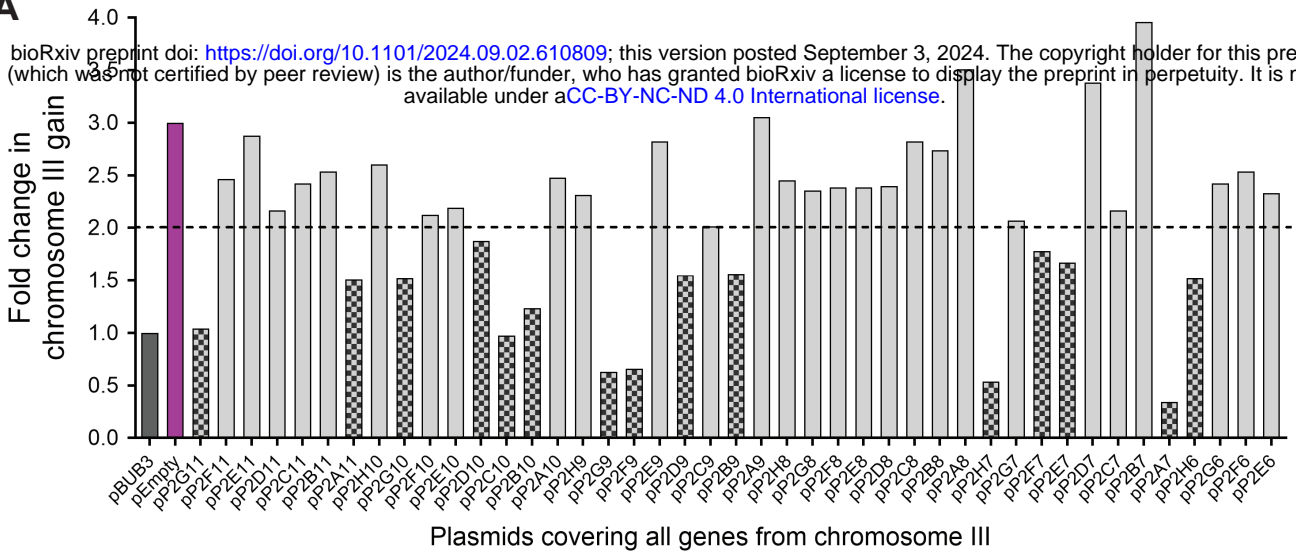
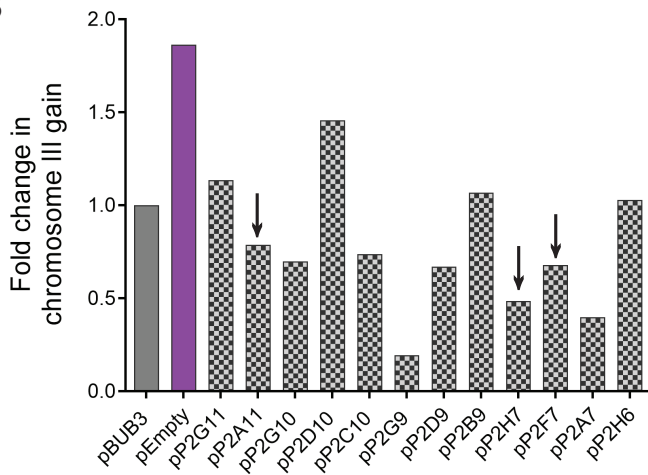
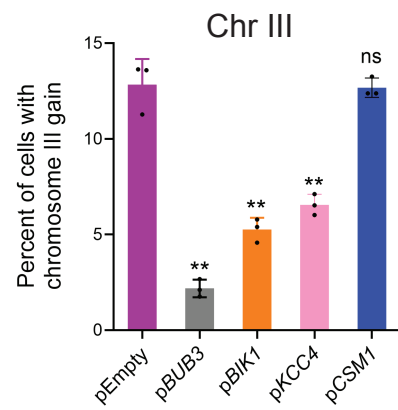
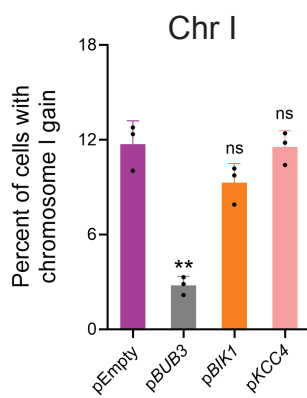
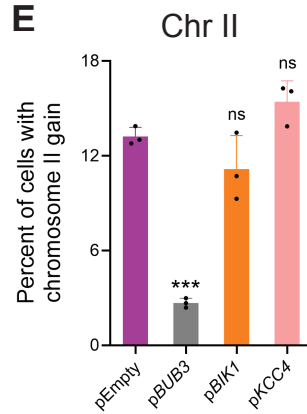
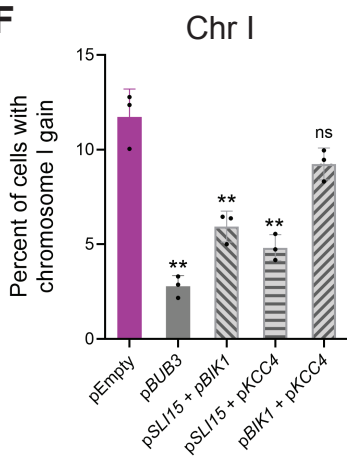
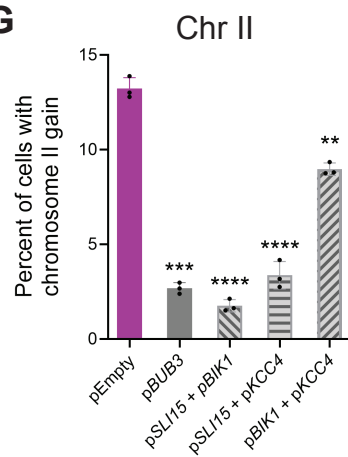
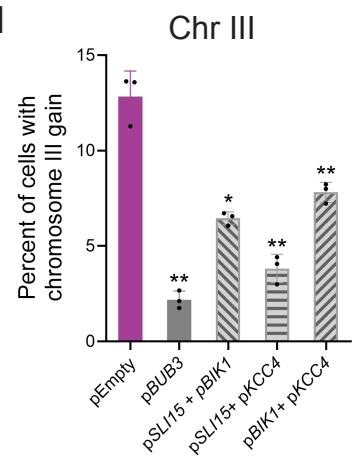
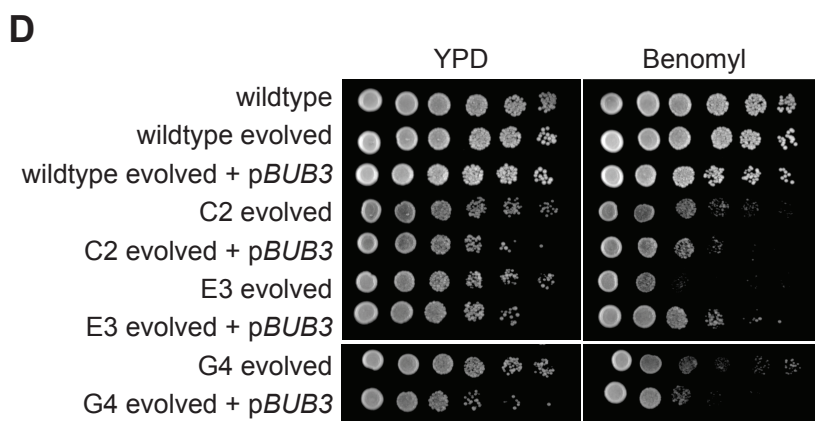
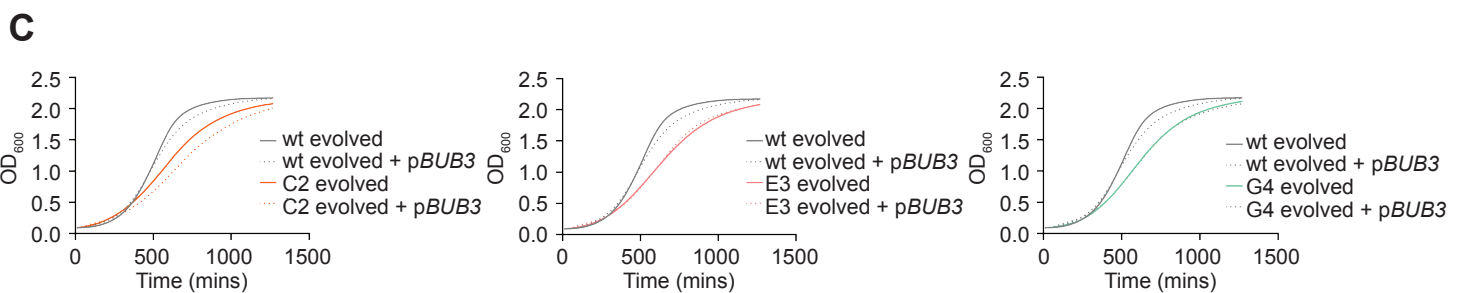
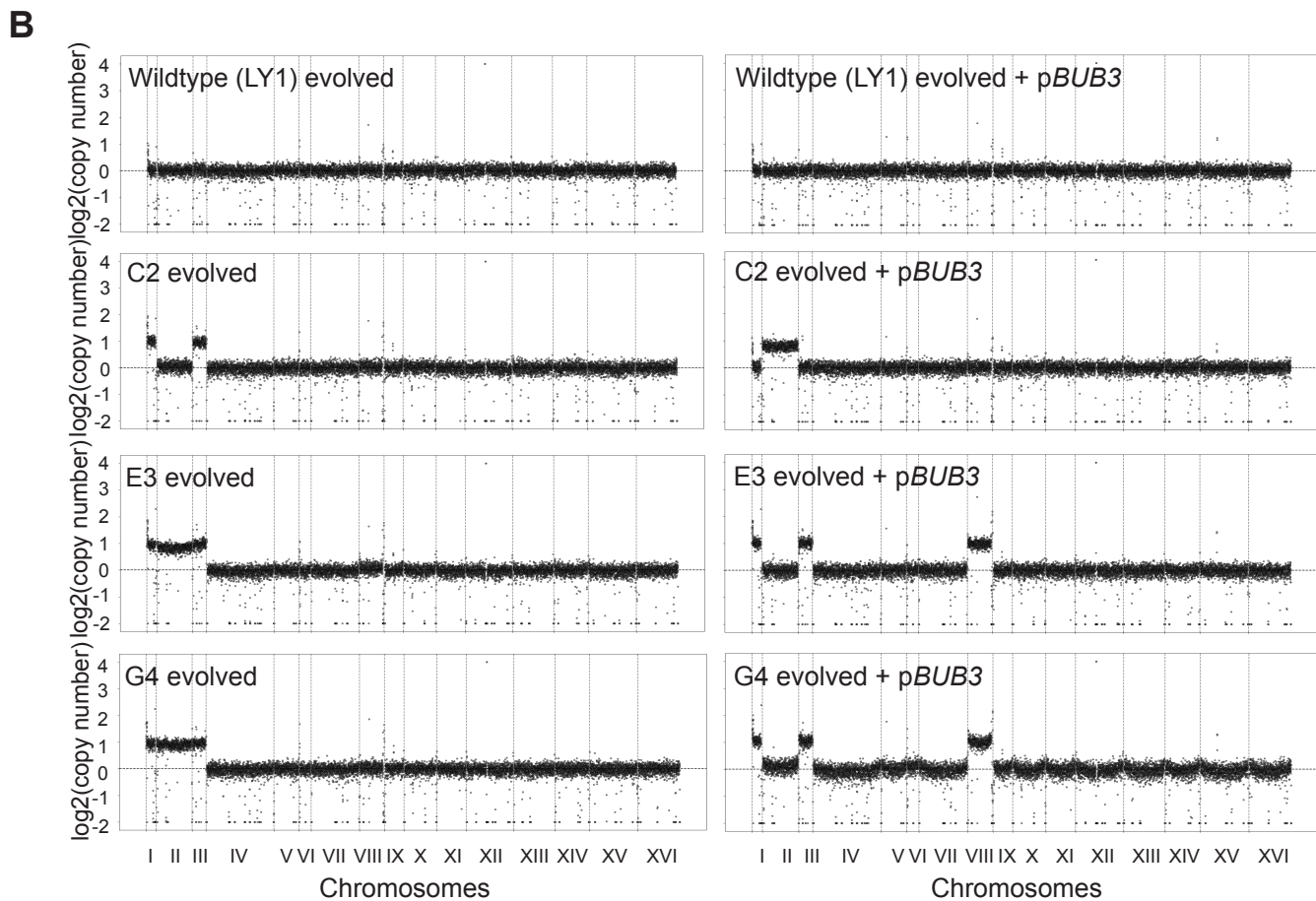
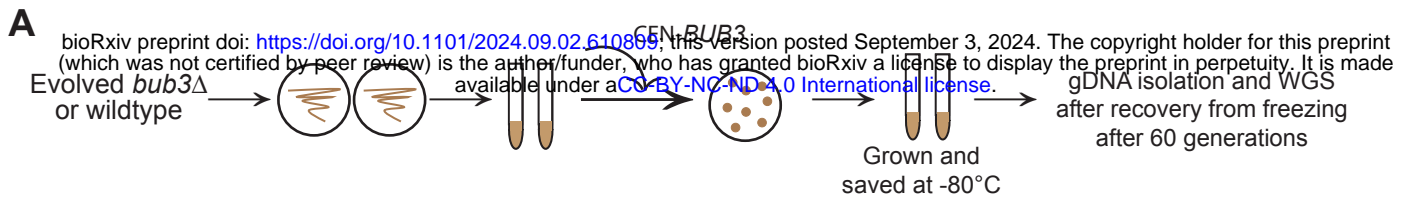
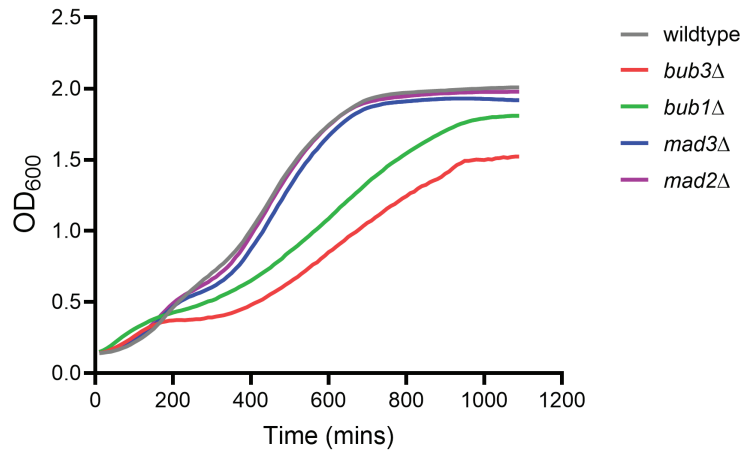
**B****C****D****E****F****G****H**

Figure 6

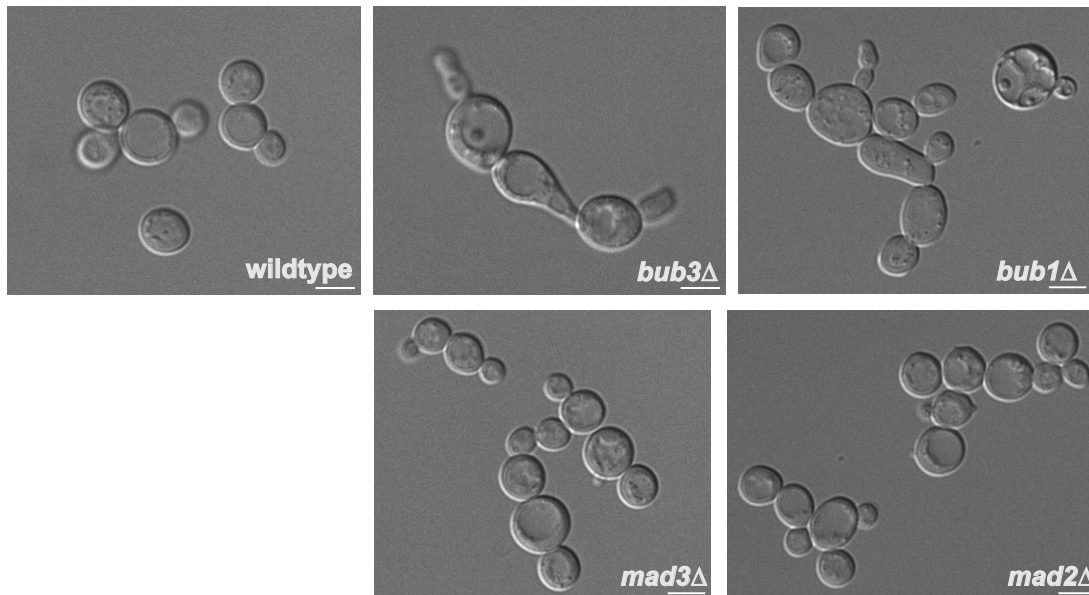
Supplementary figure 1

bioRxiv preprint doi: <https://doi.org/10.1101/2024.09.02.610809>; this version posted September 3, 2024. The copyright holder for this preprint (which was not certified by peer review) is the author/funder, who has granted bioRxiv a license to display the preprint in perpetuity. It is made available under a [CC-BY-NC-ND 4.0 International license](#).

A

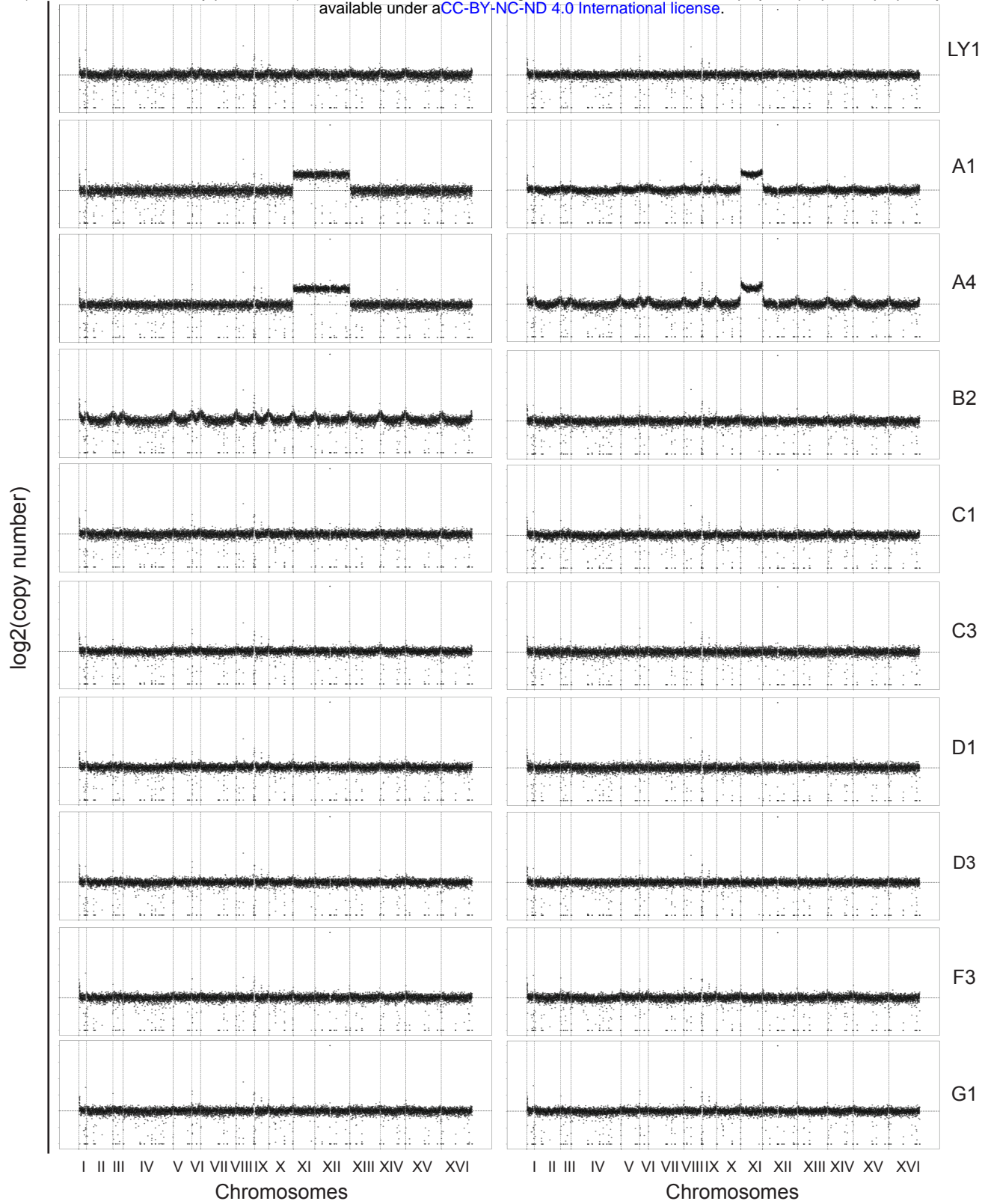


B

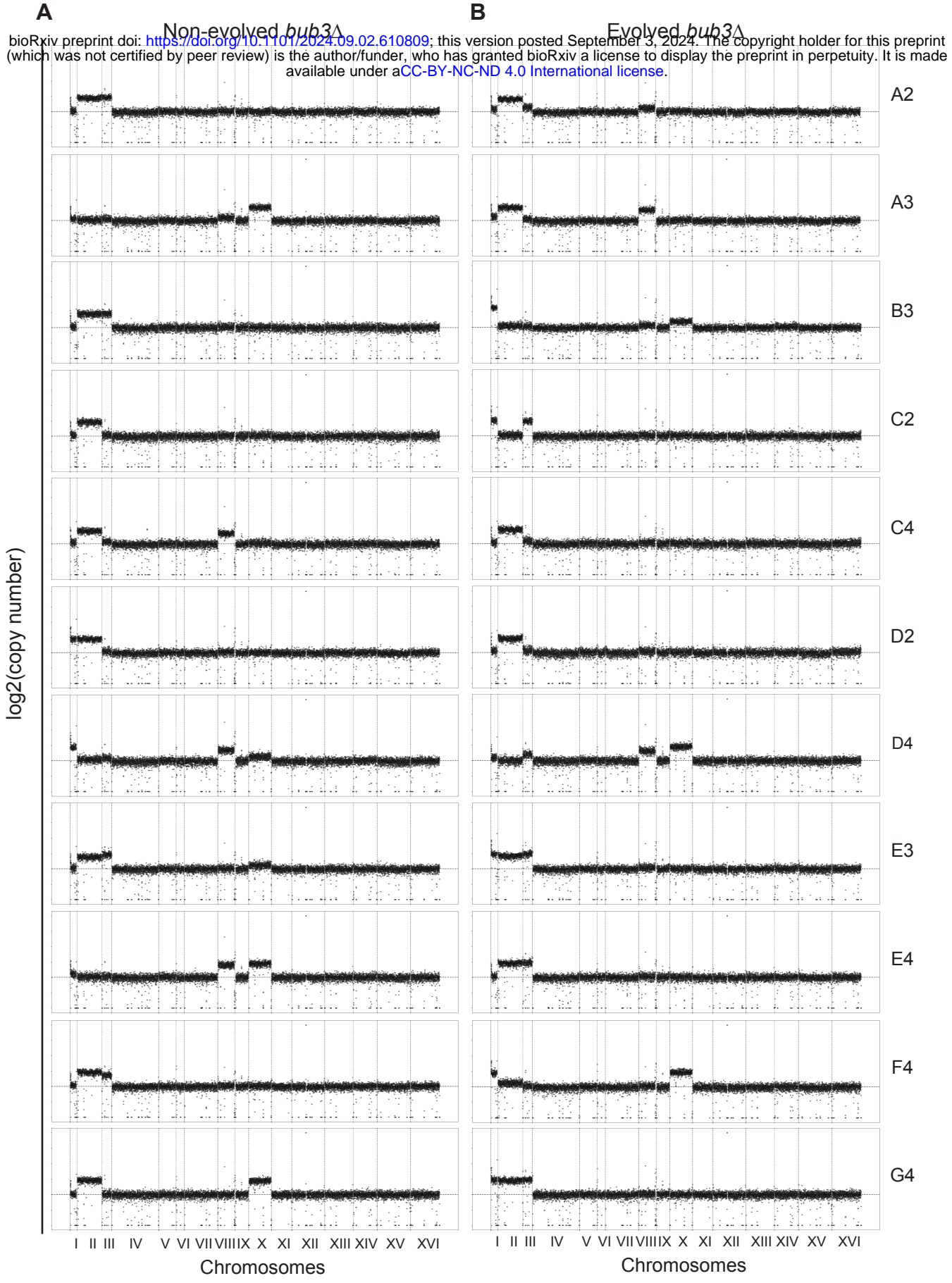


Supplementary Figure 2

A Non-evolved Wildtype **B** Evolved Wildtype
bioRxiv preprint doi: <https://doi.org/10.1101/2024.09.02.610809>; this version posted September 3, 2024. The copyright holder for this preprint (which was not certified by peer review) is the author/funder, who has granted bioRxiv a license to display the preprint in perpetuity. It is made available under a [CC-BY-NC-ND 4.0 International license](https://creativecommons.org/licenses/by-nc-nd/4.0/).

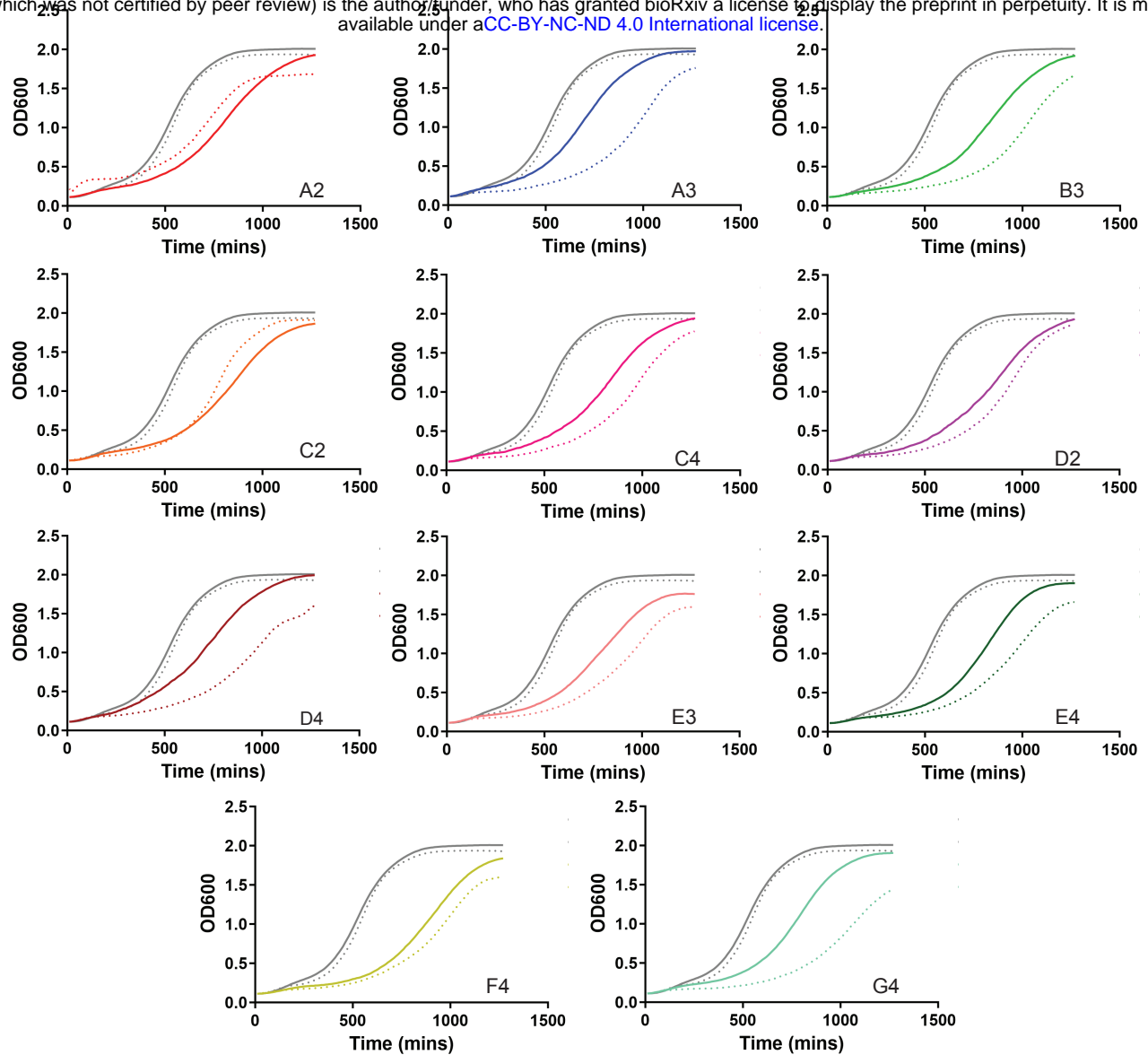


Supplementary Figure 3



Supplementary figure 4

bioRxiv preprint doi: <https://doi.org/10.1101/2024.09.02.610809>; this version posted September 3, 2024. The copyright holder for this preprint (which was not certified by peer review) is the author/funder, who has granted bioRxiv a license to display the preprint in perpetuity. It is made available under a [CC-BY-NC-ND 4.0 International license](https://creativecommons.org/licenses/by-nc-nd/4.0/).



B

		Gain of chromosomes		Growth comparison
	Haploid	non-evolved <i>bub3Δ</i>	evolved <i>bub3Δ</i>	evolved vs non-evolved
1	A2	II, III	II	+
2	A3	X	II, VIII	-
3	B3	II, III	I	-
4	C2	II	I, III	+
5	C4	II	II, VIII	-
6	D2	I, II	II	±
7	D4	I, VIII	VIII, X	-
8	E3	II, III	I, II, III	-
9	E4	VIII, X	II, III	-
10	F4	II, III	I, X	±
11	G4	II, X	I, II, III	-